

Multi-scale Processes in the Equatorial Western Pacific

Chung-Hsiung SUI¹ and Ka-Ming LAU

*Laboratory for Atmosphere, NASA/Goddard Space Flight Center
Greenbelt, MD 20771 - U.S.A.*

1. Introduction.

Recent modeling and observational studies reveal that intraseasonal oscillation (ISO) in the tropical atmosphere contains higher frequency components. Nakazawa (1989) found that convection associated with intraseasonal oscillation tends to appear in organized synoptic-scale complex systems (or called super cloud clusters SCCs). It is also known that the surface easterly trade winds over the western and central Pacific often reverse to fluctuating strong westerlies. These energetic fluctuations are known as "westerly wind bursts" (WWB). Studies by Keen (1982, 1987), Luther et al. (1983) and Murakami and Sumathipala (1988) showed that WWBs tend to be modulated by annual as well as interannual variabilities.

Lau and Chan (1988) suggested that the ISOs may act as a trigger to the development of ENSO. On the other hand, it has also been speculated that energetic WWB over the western and central Pacific may play an important role at the onset stage of ENSO (e.g. Keen, 1982, 1987; Luther et al., 1983; *etc.*). Based on the above and other studies, Lau et al. (1989) proposed that a unifying theory of the tropical climate system should include ISO, SCC and WWB as the intermediate to high frequency components. Their results show that the intermediate to high frequency variabilities are linked to the warm water region of the open ocean of the western Pacific.

The general goal of this study is to seek a better understanding of the multi-scale processes involved in the western equatorial Pacific. The results can provide an observational basis for the design of the implementation phase of the upcoming Tropical Ocean Global Atmosphere/Coupled Ocean-Atmosphere Response Experiment (TOGA/COARE) planned in 1992-1993. Most of the results of the present paper are based on data obtained from the first Special Observing Period (5 January to 4 March 1979) of the First GARP Global Experiment (FGGE).

2. Seasonal variations.

Monthly mean maps of convection and SST for December 1978, January and February 1979 are shown in figure 1. The deepest convection (represented by averaged $I_c > 2$) forms in the equatorial belt (shaded areas) and is generally found over the areas of warmest SST which are located slightly south of the equator. There are broad agreement between the area of warmest SST ($> 29^\circ\text{C}$) and regions of deep convection over the open ocean regions (160°E - 170°W). The region of warmest SST over the western Pacific expand eastward in concert with the increased area of deep convection from December to January. The center of I_c near 130° - 140°E shifts over the Gulf of Carpentaria signalling the development of the Australian monsoon.

1. NCR-NASA Resident Research Associate



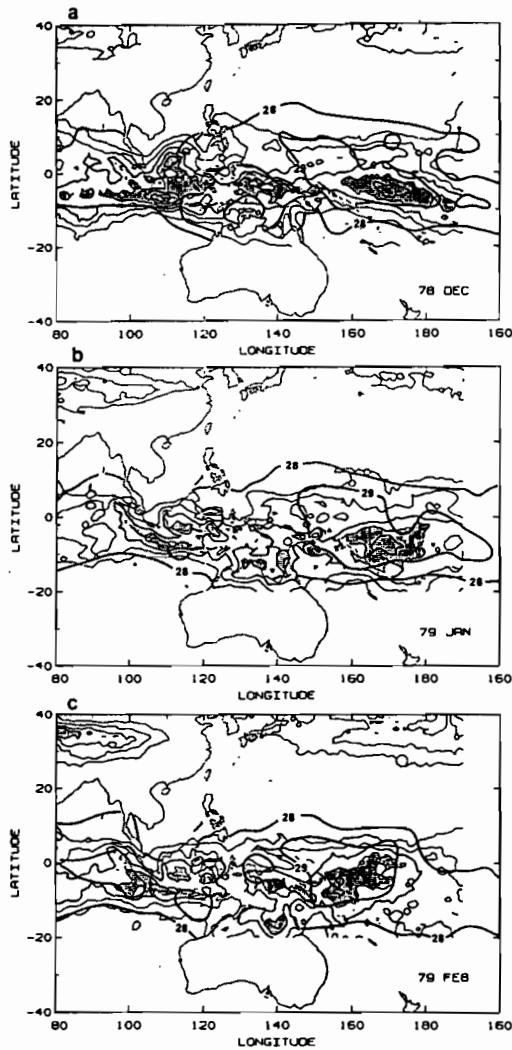


FIG.1. Monthly mean SST (heavy contour lines, interval is 1°C) and convection index, I_c (contour interval is 0.5 and the shaded regions indicate $I_c \geq 2$) for (a) December, 1978; (b) January, 1979; and (c) February, 1979.

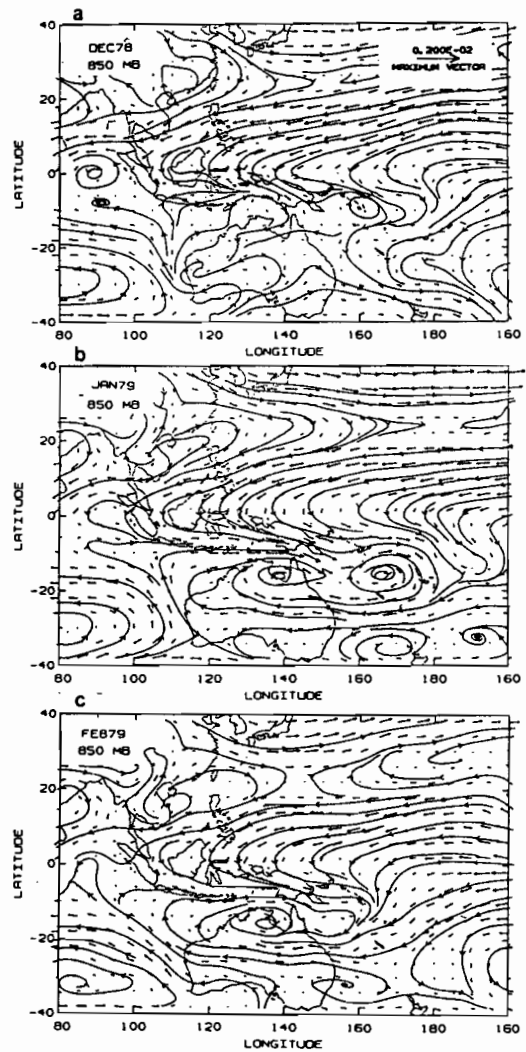


FIG.2. Monthly mean horizontal wind and streamline at 850 mb for (a) December, 1978; (b) January, 1979; and (c) February, 1979.

Corresponding to the strong convective heating, centers of equatorial cyclonic flow are formed at 850 mb (Fig.2). The 850 mb flow indicates very strong and persistent easterly wind over the western Pacific from the equator to 20°N throughout the season. The cyclonic circulation with centers over the gulf of Carpentaria and the western Pacific are most conspicuous during January associated with the development of Australian monsoon.

The onset of the Australian monsoon is often characterized by a sudden development of low-level westerlies between the equator and 10°S during late December or early January. This is clearly illustrated in figure 3 which shows the time-height distribution of averaged zonal wind between 110° and 140°E at 10°S . The sudden establishment of westerly winds in the lower troposphere started around December 22. The westerly winds persisted for over two months with a break from February 10 to 16. Easterly winds prevailed in the upper troposphere after the onset of monsoon.

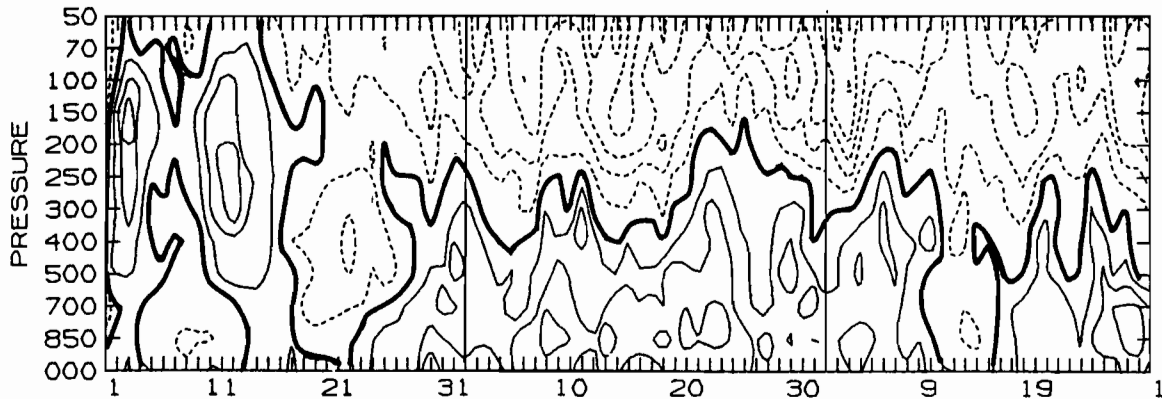


FIG.3. Time-height distribution of averaged zonal wind between 110° and 140°E at 10°S. Contour interval is 4 m s⁻¹.

Once westerlies are established in the near-equatorial trough (0°-10°S), strong convective systems tend to develop in this area. The accumulative rainfall rate at Darwin shown in figure 4 indicates that a large part of monsoon rainfall is due to a few heavy precipitation events. The first heavy precipitation occurred at December 26 at the time of the onset followed by a second event near January 2. A third event occurred around January 7 and lasted for several days. During the monsoon break (February 10-18), the cumulative curve remained essentially flat indicating very little precipitation occurred during this period.

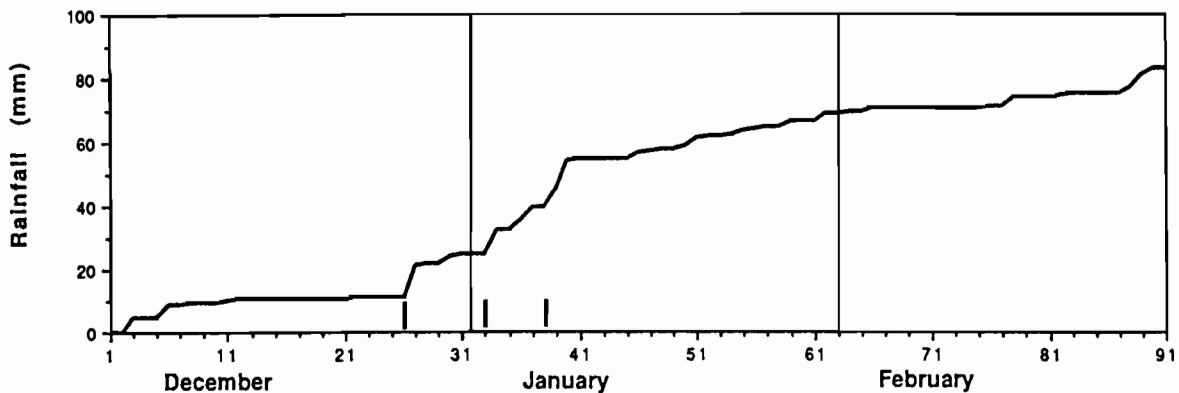


FIG.4. Accumulative rainfall at Darwin (12.42°S, 130.87°E).

3. Subseasonal scale variabilities.

During the three-month period, there are two predominant eastward-moving intraseasonal signals shown in the time-longitude section of the averaged I_c (over 4° latitude by 5° longitude grid boxes) centered at 10°S (Fig.5). These two intraseasonal disturbances consist of several "super cloud clusters". Here a SCC is loosely defined as an ensemble of deep convective clouds represented by the averaged I_c larger than certain threshold value. The threshold value is chosen as 3.5 in figure 5.

During mid-December of 1978, the first SCC is detected over the Indian Ocean near 90°E longitude (labeled A1). The disturbance moved eastward to northern Australia (120°-140°E) where a strong SCC (labeled A2 associated with the Australian monsoon) developed in late December. The average eastward-moving speed of SCC A2 is about 3.75° longitude day⁻¹. The intraseasonal disturbance was interrupted by a westward-moving SCC (labeled B1) near 160°E at January 5. The latter is first observed

near the date line and propagates westward with a phase speed of approximately 6° longitude day^{-1} . There appears to be an apparent enhancement in the convection as the two SCCs meet near 160°E . The two disturbances re-emerge after their brief encounter. SCC B1 moves westward rapidly and disappeared near 120°E after January 10 while SCC A2 continues its eastward migration while a new SCC (labeled A3) is developed downstream near the date line from 10 to 20 of January.

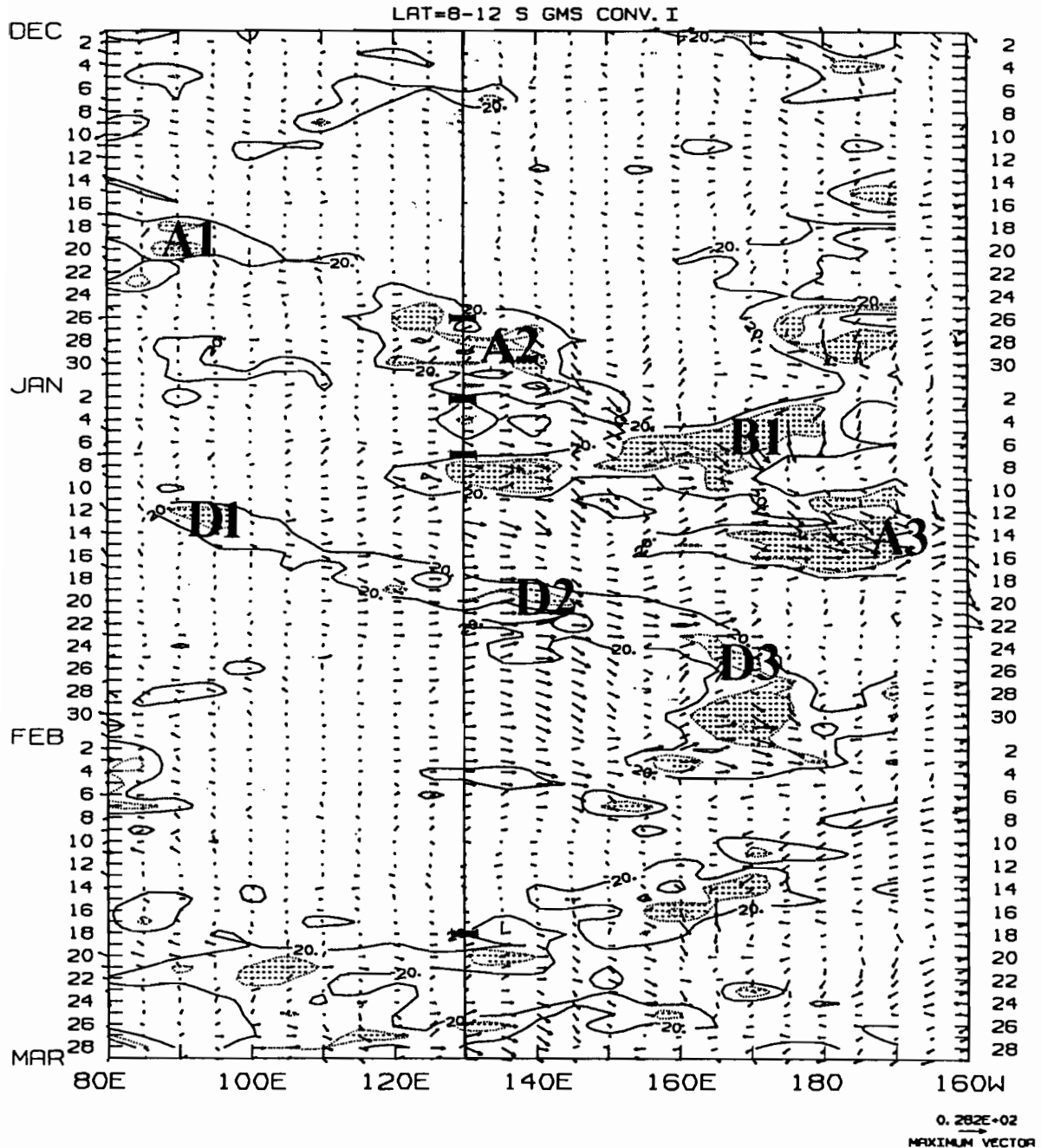


FIG.5. Time-longitude distribution of I_c and 850 mb wind at 10°S . Data resolution is 4° latitude by 5° longitude and 24 hourly. The minimum I_c plotted is 2 and contour interval is 1.5. Dotted regions indicate $I_c \geq 3.5$.

The second intraseasonal disturbance appeared at 90°E about 20 days following the first disturbance (around January 12). It maintained a continuous band of moderate convective activity from the Indian ocean to 170°E from its first inception to late January and early February. The average speed is about 6.15° longitude day⁻¹. A stationary SCC (labeled D3) was fully developed by February 1. From here on to the end of February, the centers of convection retreated westward to the maritime continent. This large scale east-west migration of convection from December to February seems to be consistent with the seasonal variation of the warm SST noted in figure 1. Thus it appears that while the ISO possesses low frequency variation of its own, it seems to be phase locked to the SST seasonal variation.

The relationship of the ISOs and the phase of the Australian monsoon is particularly interesting. A vertical line drawn along 130°E in figure 5 intersects the 2.0 Ic contour near December 26, January 2, January 7 and February 18 which coincides remarkably with the abrupt steep slopes in the cumulative rainfall time series in the vicinity of Darwin (Fig.4). Thus the large fluctuation in rain fall over Darwin during the monsoon season is not entirely a local phenomena but rather should be considered as a local manifestation of a large scale phenomenon which possesses many spatial and temporal scales.

We next examine the lower tropospheric circulation associated with the SCCs. The time-longitude section of 850 mb zonal wind at 10°S is also shown in figure 5. Over the region 120° E to 180° westerly winds were found after the onset of the Australian monsoon near the last week of December to the end of February. These westerly winds fluctuate in accord with the passage of SCCs over the region. Most notably is the episodic eastward extension of a tongue of strong westerly winds to the western Pacific during January 12-18 and January 30 to February 4 respectively. The location and duration of these westerly events are consistent with those for WWBs defined by Keen (1987). These two events will be referred to as WWB1 and WWB2 hereafter. Maximum westerly winds of over 25 ms⁻¹ are found during the peak for both events. The region of maximum westerly wind appear to agree very well with centers of the SCCs. The westerly wind leading up to the WWB1 can be traced to the onset of the Australian monsoon. For WWB2 the westerly wind axis can be tracked to 110°E near January 16. One of the most important message from figure 5 is that the WWBs and SCCs are not isolated or random events that all happen to be found in the western Pacific, but rather they are parts of a closely related and interacting system of many different scales.

4. Propagation and structure of ISO in relation to WWB.

In this section we investigate the large scale circulation and convection pattern associated with the ISOs leading up to the maximum low level westerly wind in WWB1 and WWB2. The important features of sequence of events for WWB1 and WWB2 are similar. For brevity, only the WWB2 is discussed here. Figures 6 a-d show the horizontal distribution of Ic and 850 mb wind at every 5 day intervals starting from January 15 till January 30. A five-day equal-weight averaging is applied to the data to emphasize the ISO signal.

The systematic eastward propagation of SCCs D1, D2, D3 from 100°E at January 15 (Fig. 6a) to 165°E at January 25 (Fig.6c) is obvious. Between January 25-30, the SCC appears quasi-stationary. This sequence should be compared with that shown in figure 5. Strong westerly winds are often found along 10°S sandwiched between two cyclonic inflow regions to the west of the SCC. It is noted that the region of westerly wind is quite extensive in longitude but the convection appear to be confined mostly to the eastern terminus of the region of westerlies.

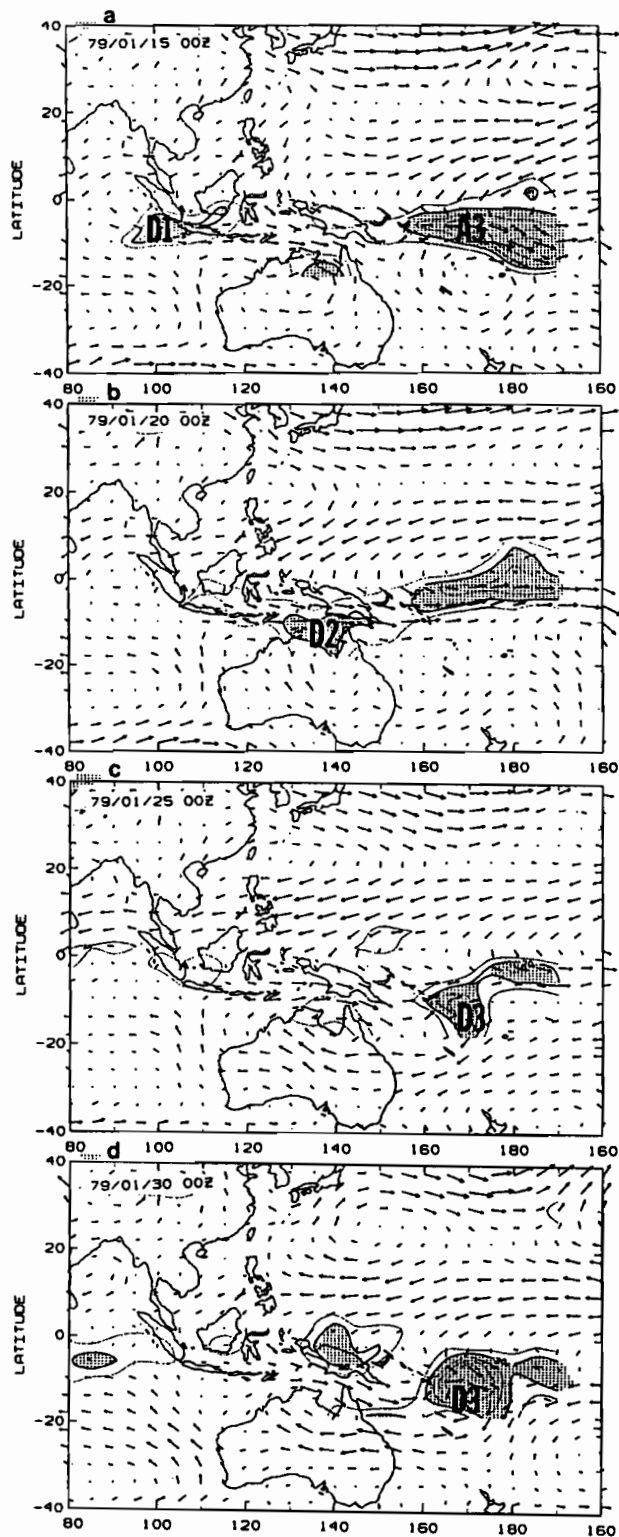


FIG.6. Horizontal distributions of I_c and 850 mb wind averaged over five day periods centered at (a) 00Z 15 January, 1979; (b) 00Z 20 January, 1979; (c) 00Z 25 January, 1979; and (d) 00Z 30 January, 1979. Contour interval of I_c is 0.5 and the shaded regions indicate $I_c \geq 2$.

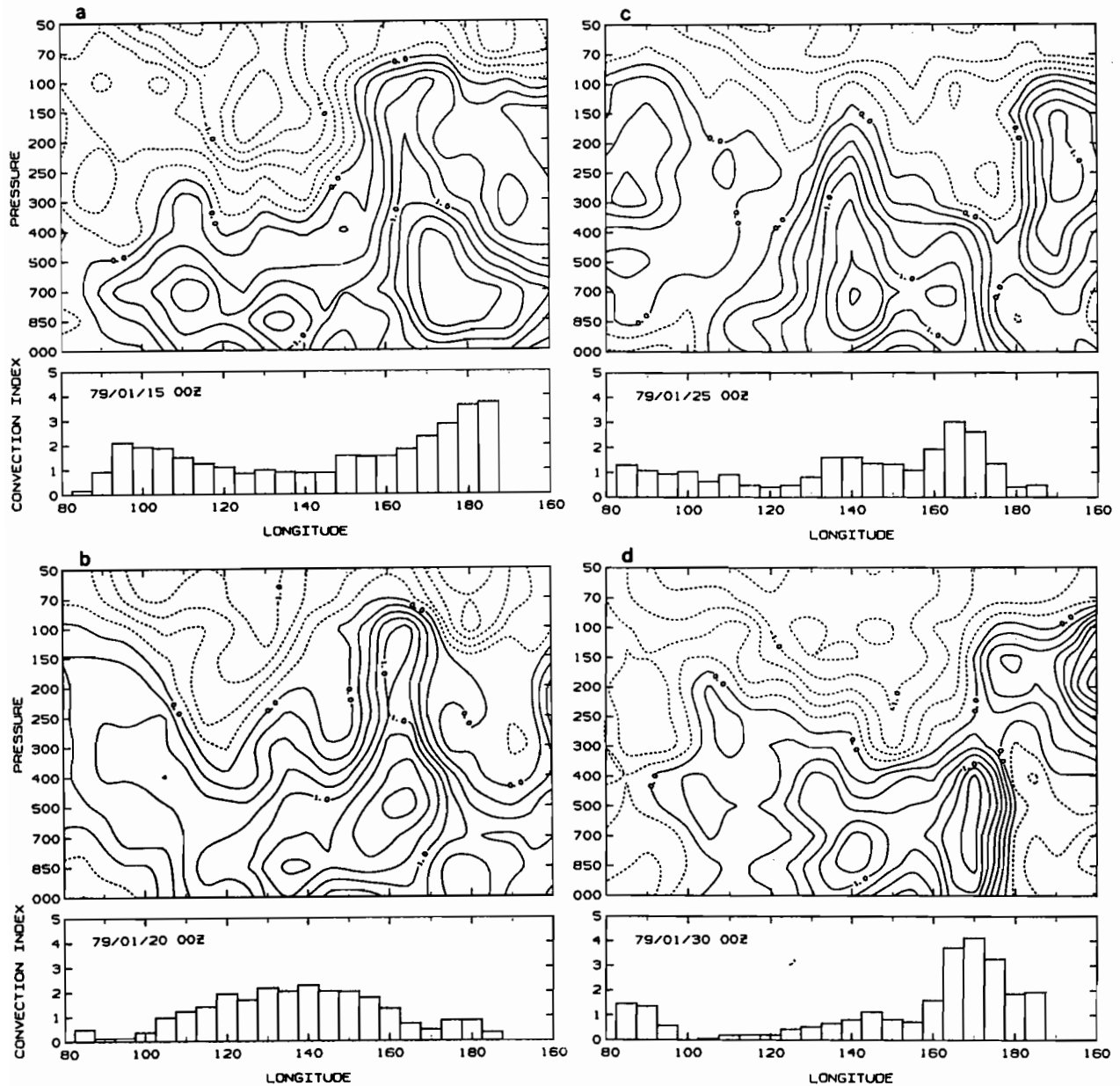


FIG.7. Vertical-zonal distribution of five-day mean zonal wind (upper) and zonal distribution of I_c (lower) along 10°S , respectively, for (a) 00Z 15 January, 1979; (b) 00Z 20 January, 1979; (c) 00Z 25 January, 1979; and (d) 00Z 30 January, 1979.

The vertical distribution of zonal wind along 10°S for WWB2 is shown in figures 7 a-d. The most conspicuous feature shown in figure 7 is the eastward moving baroclinic structure associated with the ISO. As noted before on January 15, major convective centers (D1 and A3) are found in the two extreme ends of the westerly wind belt. This period corresponds to the maximum development of WWB1 and the beginning phase of WWB2. We shall focus on the development associated with D1 in the following

discussions. The strong westerly wind in the lower troposphere is capped by easterly wind above 400 mb near 110° (Fig. 7a). The convective center D1 moves to 140° E at January 20 with the low level westerlies consolidating over a rather extensive region of above-normal convection. At about 160°E, the westerly wind extends throughout the troposphere and appears to have an equivalent barotropic structure above 700 mb with the upper troposphere westerlies. At this point, while the convection appears to be related to the low level westerly wind, it does not appear to have a strong control on the large scale circulation as evidenced by the presence of the transient barotropic structure of the disturbance decoupled from the region of enhanced convection. As the convection moves to 165°E 5 days later, it begins to intensify. The direct control of convection on the circulation can be seen by the marked change in the vertical structure of the zonal wind. Here, maximum low-level westerly wind is found at low level and to the west of the convection center D3. The low level westerlies has a wavy structure with two maxima separated by about 20° in longitude. A region of weak easterly wind appears below 700 mb east of the date line indicating strong low level convergence near 170°E. The upper level easterly wind over the region of the SCC suggests a first baroclinic mode with a weak westward tilt with height. This strongly signals an interaction between the circulation and latent heating for propagating unstable modes as discussed in Lau and Peng (1987)'s theory of ISO. At the peak of WWB2 (Fig. 7d), ISO becomes stationary (see Fig.5). The vertical structure of the zonal wind indicates a very strong low level convergence with the strongest westerly wind over the center of the SCC D3 near the date line. The distribution of zonal wind in the vertical plane and the absence of a vertical tilt in the wave axis are consistent with the appearance of stationary modes forced by latent heating (cf. Chang and Lim, 1988).

5. Summary and Discussion.

In this study, we have systematically analyzed the features of multi-scale processes over the western Pacific region using observations collected during winter of the FGGE year. Generally speaking, intraseasonal oscillations are composed of a series of cloud clusters. These cloud clusters tend to organize into a synoptic scale (called super cloud clusters) when subject to favorable large-scale conditions like in the monsoon trough region or over the warm pool of the ocean. The circulation induced by convective heating is characterized by strong low-level convergent flow with asymmetric zonal winds, i.e. stronger westerly flow to the west of heating and weaker easterly flow to the east of heating.

Approaching the warm pool of the western Pacific, eastward-moving SCCs tend to slow down and intensify. Besides eastward-moving SCCs, westward-moving SCCs are also excited over the warm pool in the western Pacific. These SCCs have strong low-level cyclonic vorticity and dissipate quickly once move out of the source region. These features are consistent with the "Rossby wave-shed off" within the mobile Wave-CISK mechanism as suggested in Lau et al. (1989).

The frequency and intensity of SCCs and westerly wind bursts revealed in this study suggest that it is important to include them in the study of low-frequency climate variability. It is also essential to understand and simulate the basic equilibrium state of the oceanic mixed layer and their changes to the impact of SCCs and westerly wind bursts in order to obtain a realistic feedback between the ocean and the atmosphere.

REFERENCES

- Chang, C.P., and H. Lim, 1988: Kelvin wave-CISK: a possible mechanism for the 30-50 day oscillations. *J. Atmos. Sci.*, **45**, 1709-1720.
- Keen, R.A., 1982: The role of cross-equatorial tropical cyclone pairs in the southern oscillation. *Mon. Wea. Rev.*, **110**, 1405-1416.
- Keen, R.A., 1987: Equatorial westerlies and Southern Oscillation. Proceedings of the US TOGA western Pacific air-sea interaction workshop. September 16-18, Honolulu, Hawaii.
- Lau, K.M., and P. Chan, 1988: Intraseasonal and interannual variations of tropical convection: A possible link between the 40-50 day oscillation and ENSO? *Mon. Wea. Rev.*, **45**, 506-521.
- Lau, K.M., and L. Peng, 1987: Origin of low frequency (intraseasonal) oscillations in the tropical atmosphere. Part. I: the basic theory. *J. Atmos. Sci.*, **44**, 950-972.
- Lau, K.M., L. Peng, C.H. Sui and T. Nakazawa, 1989: Super cloud clusters, westerly wind burst, 30-60 day oscillations and ENSO: An emerging unified theory. (submitted to *J. Meteor. Soc. Japan*).
- Luther, D.S., D.E. Harrison and R.A. Knox, 1983: Zonal winds in the central equatorial Pacific and El Nino. *Science*, **222**, 327-330.
- Murakami, T., L.X. Chen and A. Xie, 1986: Relationship among seasonal cycles, low-frequency oscillations and transient disturbances as revealed from Outgoing Longwave radiation data. *Mon. Wea. Rev.*, **114**, 1456-1465.
- Murakami, T., and W.L. Sumathipala, 1988: Westerly bursts during the 1982/1983 ENSO. To be submitted to *J. of Climate*.
- Nakazawa, T. 1988: Tropical super clusters with intraseasonal variations over the western Pacific. *J. Meteor. Soc. Japan.*, **66**, 823-839.

**WESTERN PACIFIC INTERNATIONAL MEETING
AND WORKSHOP ON TOGA COARE**

Nouméa, New Caledonia

May 24-30, 1989

PROCEEDINGS

edited by

Joël Picaut *

Roger Lukas **

Thierry Delcroix *

* ORSTOM, Nouméa, New Caledonia

** JIMAR, University of Hawaii, U.S.A.

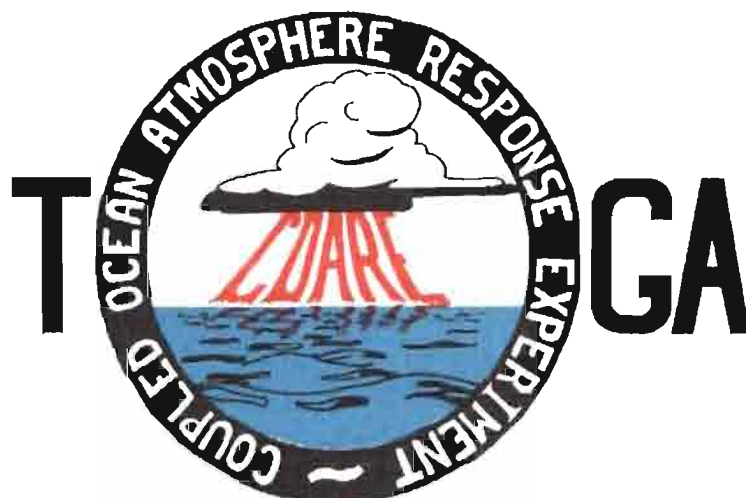


TABLE OF CONTENTS

ABSTRACT	i
RESUME	iii
ACKNOWLEDGMENTS	vi
INTRODUCTION	
1. Motivation	1
2. Structure	2
LIST OF PARTICIPANTS	5
AGENDA	7
WORKSHOP REPORT	
1. Introduction	19
2. Working group discussions, recommendations, and plans	20
a. Air-Sea Fluxes and Boundary Layer Processes	20
b. Regional Scale Atmospheric Circulation and Waves	24
c. Regional Scale Oceanic Circulation and Waves	30
3. Related programs	35
a. NASA Ocean Processes and Satellite Missions	35
b. Tropical Rainfall Measuring Mission	37
c. Typhoon Motion Program	39
d. World Ocean Circulation Experiment	39
4. Presentations on related technology	40
5. National reports	40
6. Meeting of the International Ad Hoc Committee on TOGA COARE	40
APPENDIX: WORKSHOP RELATED PAPERS	
Robert A. Weller and David S. Hosom: Improved Meteorological Measurements from Buoys and Ships for the World Ocean Circulation Experiment	45
Peter H. Hildebrand: Flux Measurement using Aircraft and Radars	57
Walter F. Dabberdt, Hale Cole, K. Gage, W. Ecklund and W.L. Smith: Determination of Boundary-Layer Fluxes with an Integrated Sounding System	81

MEETING COLLECTED PAPERS

WATER MASSES, SEA SURFACE TOPOGRAPHY, AND CIRCULATION

Klaus Wyrtki: Some Thoughts about the West Pacific Warm Pool	99
Jean René Donguy, Gary Meyers, and Eric Lindstrom: Comparison of the Results of two West Pacific Oceanographic Expeditions FOC (1971) and WEPOCS (1985-86)	111
Dunxin Hu, and Maochang Cui: The Western Boundary Current in the Far Western Pacific Ocean	123
Peter Hacker, Eric Firing, Roger Lukas, Philipp L. Richardson, and Curtis A. Collins: Observations of the Low-latitude Western Boundary Circulation in the Pacific during WEPOCS III	135
Stephen P. Murray, John Kindle, Dharma Arief, and Harley Hurlburt: Comparison of Observations and Numerical Model Results in the Indonesian Throughflow Region	145
Christian Henin: Thermohaline Structure Variability along 165°E in the Western Tropical Pacific Ocean (January 1984 - January 1989)	155
David J. Webb, and Brian A. King: Preliminary Results from Charles Darwin Cruise 34A in the Western Equatorial Pacific	165
Warren B. White, Nicholas Graham, and Chang-Kou Tai: Reflection of Annual Rossby Waves at The Maritime Western Boundary of the Tropical Pacific	173
William S. Kessler: Observations of Long Rossby Waves in the Northern Tropical Pacific	185
Eric Firing, and Jiang Songnian: Variable Currents in the Western Pacific Measured During the US/PRC Bilateral Air-Sea Interaction Program and WEPOCS	205
John S. Godfrey, and A. Weaver: Why are there Such Strong Steric Height Gradients off Western Australia ?	215
John M. Toole, R.C. Millard, Z. Wang, and S. Pu: Observations of the Pacific North Equatorial Current Bifurcation at the Philippine Coast	223

EL NINO/SOUTHERN OSCILLATION 1986-87

Gary Meyers, Rick Bailey, Eric Lindstrom, and Helen Phillips: Air/Sea Interaction in the Western Tropical Pacific Ocean during 1982/83 and 1986/87	229
Laury Miller, and Robert Cheney: GEOSAT Observations of Sea Level in the Tropical Pacific and Indian Oceans during the 1986-87 El Nino Event	247
Thierry Delcroix, Gérard Eldin, and Joël Picaut: GEOSAT Sea Level Anomalies in the Western Equatorial Pacific during the 1986-87 El Nino, Elucidated as Equatorial Kelvin and Rossby Waves	259
Gérard Eldin, and Thierry Delcroix: Vertical Thermal Structure Variability along 165°E during the 1986-87 ENSO Event	269
Michael J. McPhaden: On the Relationship between Winds and Upper Ocean Temperature Variability in the Western Equatorial Pacific	283

John S. Godfrey, K. Ridgway, Gary Meyers, and Rick Bailey: Sea Level and Thermal Response to the 1986-87 ENSO Event in the Far Western Pacific	291
Joël Picaut, Bruno Camusat, Thierry Delcroix, Michael J. McPhaden, and Antonio J. Busalacchi: Surface Equatorial Flow Anomalies in the Pacific Ocean during the 1986-87 ENSO using GEOSAT Altimeter Data	301

THEORETICAL AND MODELING STUDIES OF ENSO AND RELATED PROCESSES

Julian P. McCreary, Jr.: An Overview of Coupled Ocean-Atmosphere Models of El Nino and the Southern Oscillation	313
Kensuke Takeuchi: On Warm Rossby Waves and their Relations to ENSO Events	329
Yves du Penhoat, and Mark A. Cane: Effect of Low Latitude Western Boundary Gaps on the Reflection of Equatorial Motions	335
Harley Hurlburt, John Kindle, E. Joseph Metzger, and Alan Wallcraft: Results from a Global Ocean Model in the Western Tropical Pacific	343
John C. Kindle, Harley E. Hurlburt, and E. Joseph Metzger: On the Seasonal and Interannual Variability of the Pacific to Indian Ocean Throughflow	355
Antonio J. Busalacchi, Michael J. McPhaden, Joël Picaut, and Scott Springer: Uncertainties in Tropical Pacific Ocean Simulations: The Seasonal and Interannual Sea Level Response to Three Analyses of the Surface Wind Field	367
Stephen E. Zebiak: Intraseasonal Variability - A Critical Component of ENSO ?	379
Akimasa Sumi: Behavior of Convective Activity over the "Jovian-type" Aqua-Planet Experiments	389
Ka-Ming Lau: Dynamics of Multi-Scale Interactions Relevant to ENSO	397
Pecheng C. Chu and Roland W. Garwood, Jr.: Hydrological Effects on the Air-Ocean Coupled System	407
Sam F. Jacobellis, and Richard C.J. Somerville: A one Dimensional Coupled Air-Sea Model for Diagnostic Studies during TOGA-COARE	419
Allan J. Clarke: On the Reflection and Transmission of Low Frequency Energy at the Irregular Western Pacific Ocean Boundary - a Preliminary Report	423
Roland W. Garwood, Jr., Pecheng C. Chu, Peter Muller, and Niklas Schneider: Equatorial Entrainment Zone : the Diurnal Cycle	435
Peter R. Gent: A New Ocean GCM for Tropical Ocean and ENSO Studies	445
Wasito Hadi, and Nuraini: The Steady State Response of Indonesian Sea to a Steady Wind Field	451
Pedro Ripa: Instability Conditions and Energetics in the Equatorial Pacific	457
Lewis M. Rothstein: Mixed Layer Modelling in the Western Equatorial Pacific Ocean	465
Neville R. Smith: An Oceanic Subsurface Thermal Analysis Scheme with Objective Quality Control	475
Duane E. Stevens, Qi Hu, Graeme Stephens, and David Randall: The hydrological Cycle of the Intraseasonal Oscillation	485
Peter J. Webster, Hai-Ru Chang, and Chidong Zhang: Transmission Characteristics of the Dynamic Response to Episodic Forcing in the Warm Pool Regions of the Tropical Oceans	493

MOMENTUM, HEAT, AND MOISTURE FLUXES BETWEEN ATMOSPHERE AND OCEAN

W. Timothy Liu: An Overview of Bulk Parametrization and Remote Sensing of Latent Heat Flux in the Tropical Ocean	513
E. Frank Bradley, Peter A. Coppin, and John S. Godfrey: Measurements of Heat and Moisture Fluxes from the Western Tropical Pacific Ocean	523
Richard W. Reynolds, and Ants Leetmaa: Evaluation of NMC's Operational Surface Fluxes in the Tropical Pacific	535
Stanley P. Hayes, Michael J. McPhaden, John M. Wallace, and Joël Picaut: The Influence of Sea-Surface Temperature on Surface Wind in the Equatorial Pacific Ocean	543
T.D. Keenan, and Richard E. Carbone: A Preliminary Morphology of Precipitation Systems In Tropical Northern Australia	549
Phillip A. Arkin: Estimation of Large-Scale Oceanic Rainfall for TOGA	561
Catherine Gautier, and Robert Frouin: Surface Radiation Processes in the Tropical Pacific	571
Thierry Delcroix, and Christian Henin: Mechanisms of Subsurface Thermal Structure and Sea Surface Thermo-Haline Variabilities in the South Western Tropical Pacific during 1979-85 - A Preliminary Report	581
Greg. J. Holland, T.D. Keenan, and M.J. Manton: Observations from the Maritime Continent : Darwin, Australia	591
Roger Lukas: Observations of Air-Sea Interactions in the Western Pacific Warm Pool during WEPOCS	599
M. Nunez, and K. Michael: Satellite Derivation of Ocean-Atmosphere Heat Fluxes in a Tropical Environment	611

EMPIRICAL STUDIES OF ENSO AND SHORT-TERM CLIMATE VARIABILITY

Klaus M. Weickmann: Convection and Circulation Anomalies over the Oceanic Warm Pool during 1981-1982	623
Claire Perigaud: Instability Waves in the Tropical Pacific Observed with GEOSAT	637
Ryuichi Kawamura: Intraseasonal and Interannual Modes of Atmosphere-Ocean System Over the Tropical Western Pacific	649
David Gutzler, and Tamara M. Wood: Observed Structure of Convective Anomalies	659
Siri Jodha Khalsa: Remote Sensing of Atmospheric Thermodynamics in the Tropics	665
Bingrong Xu: Some Features of the Western Tropical Pacific: Surface Wind Field and its Influence on the Upper Ocean Thermal Structure	677
Bret A. Mullan: Influence of Southern Oscillation on New Zealand Weather	687
Kenneth S. Gage, Ben Basley, Warner Ecklund, D.A. Carter, and John R. McAfee: Wind Profiler Related Research in the Tropical Pacific	699
John Joseph Bates: Signature of a West Wind Convective Event in SSM/I Data	711
David S. Gutzler: Seasonal and Interannual Variability of the Madden-Julian Oscillation	723
Marie-Hélène Radenac: Fine Structure Variability in the Equatorial Western Pacific Ocean	735
George C. Reid, Kenneth S. Gage, and John R. McAfee: The Climatology of the Western Tropical Pacific: Analysis of the Radiosonde Data Base	741

Chung-Hsiung Sui, and Ka-Ming Lau: Multi-Scale Processes in the Equatorial Western Pacific	747
Stephen E. Zebiak: Diagnostic Studies of Pacific Surface Winds	757

MISCELLANEOUS

Rick J. Bailey, Helene E. Phillips, and Gary Meyers: Relevance to TOGA of Systematic XBT Errors	775
Jean Blanchot, Robert Le Borgne, Aubert Le Bouteiller, and Martine Rodier: ENSO Events and Consequences on Nutrient, Planktonic Biomass, and Production in the Western Tropical Pacific Ocean	785
Yves Dandonneau: Abnormal Bloom of Phytoplankton around 10°N in the Western Pacific during the 1982-83 ENSO	791
Cécile Dupouy: Sea Surface Chlorophyll Concentration in the South Western Tropical Pacific, as seen from NIMBUS Coastal Zone Color Scanner from 1979 to 1984 (New Caledonia and Vanuatu)	803
Michael Szabados, and Darren Wright: Field Evaluation of Real-Time XBT Systems	811
Pierre Rual: For a Better XBT Bathy-Message: Onboard Quality Control, plus a New Data Reduction Method	823